Journal of
MATERIALS RESEARCH

Diffused phase transition in fine-grained bismuth vanadate ceramics

K. Shantha and K.B.R. Varma[a)]
Materials Research Centre, Indian Institute of Science, Bangalore-560 012, India

(Received 18 November 1998; accepted 13 September 1999)

Nanocrystalline powders of ferroelectric bismuth vanadate, $Bi_4V_2O_{11}$ (n-BiV), with crystallite size less than 50 nm, were obtained by mechanical milling of a stoichiometric mixture of bismuth oxide and vanadium pentoxide. The n-BiV powders on sintering yielded high-density, fine-grained ceramics with improved dielectric and polar characteristics. Dielectric studies on samples obtained from milled powders indicated that the ferroelectric-to-paraelectric phase transition temperature is strongly frequency dependent. The Curie–Weiss law is found to be valid only at a temperature away from the transition temperature, confirming the diffused nature of the transition, which is attributed to the presence of compositional inhomogeneity, because of partial reduction of vanadium.

I. INTRODUCTION

Bismuth vanadate, $Bi_4V_2O_{11}$ (BiV), is an important member of the Aurivillius family of bismuth-based layered-structured oxides, consisting of $(Bi_2O_2)^{2+}$ layers interleaved with perovskite-like sheets of $(VO_{3.5}\square_{0.5})^{2-}$.[1,2] BiV exhibits two polymorphs $\alpha \rightarrow \beta$ (720 K) and $\beta \rightarrow \gamma$ (840 K).[3] The most attractive feature of this compound is its strong polar response[4,5] and high ionic mobility,[6] which are generally incompatible in most ferroelectrics. It finds a wide variety of applications in catalysts,[7] gas sensors,[8] and solid-state electrolytes,[9] as electrode materials for lithium rechargeable batteries[10] and pyroelectric detectors.[4] It is known that the dielectric and polar properties and the nature of phase transitions in ceramics are very sensitive to their microstructure.[11,12] As a result, studies concerning the effects of grain size on the dielectric and polar properties of ferroelectric materials are interesting from both scientific and technological points of view. In recent years, there has been an increasing interest in the field of processing of ceramic components from ultrafine-grained powders which exhibit improved sinterability and hence yield fine-grained ceramics with improved electrical properties.[13–16] Hence, we have fabricated fine-grained ceramics from nanopowders of BiV (n-BiV) and studied their dielectric and polar properties. Some of the interesting observations that were made during our investigations are reported in this paper.

The main chemical complexity associated with BiV is related to the ability of V^{5+} to be easily reduced to V^{4+}, during thermal treatment or when the oxygen partial pressure is modified. This leads to the formation of mixed valence phases of the form $(Bi_2O_2)_2$ $(V^{4+}_{\ x}V^{5+}_{\ 2-x})$ O_{7-x}, where x varies between 0 and 0.33, i.e., all phases between $Bi_4V_2O_{11}$ and $Bi_4V_2O_{10.66}$ can exist.[17] So it is very difficult to obtain fully unreduced-BiV by normal preparation, and the extent of vanadium reduction depends on the specific preparation conditions. Some of the unusual properties of fine-grained BiV ceramics were found to be associated with the nonstoichiometry arising out of the partial vanadium reduction in these samples. Hence, a systematic investigation into the influence of nonstoichiometry on the transition temperatures and the electrical properties was taken up, the results of which are elucidated in this paper.

II. EXPERIMENTAL

Conventional solid-state reaction route of preparing BiV, by heating a stoichiometric mixture of reagent grade Bi_2O_3 and V_2O_5, initially at 770 K and then at 1070 K for 24 h with intermediate grinding steps, was found to yield micron-sized (m) BiV powders. Nanocrystalline bismuth vanadate powders were prepared by mechanochemical synthesis. For this purpose, a stoichiometric mixture of commercial powders of Bi_2O_3 (>99.9% pure, Aldrich) and V_2O_5 (>99.9% pure, Johnson Matthey) were mixed in acetone and ball milled using a Laboratory Centrifugal ballmill (Fritsh Pulverisette 6).

The x-ray powder diffraction (XRD) studies were done using an x-ray diffractometer (Scintag) with Cu K_α radiation. The densities of the sintered ceramics were

a)Address all correspondence to this author.
e-mail: kbrvarma@mrc.iisc.ernet.in

determined by the liquid displacement method, using xylene (whose density is 0.87 gm/cm^3) as the liquid media. The impedance, capacitance, and the dielectric loss were monitored, as functions of both frequency (100 Hz–10 MHz) and temperature (300–800 K), using an impedance/gain-phase analyzer (HP 4194A) at a signal strength of 0.5 Vrms, in conjunction with an indigenously built temperature variation cell. The dielectric constants of all the samples were corrected for porosity by using the equation governing parallel mixing:

$$\epsilon_r = \epsilon_{robs} (d_{th}/d_{obs}) \quad ,$$

where ϵ_{robs} is the measured dielectric constant, d_{th} is the theoretical density, and d_{obs} is the measured density. Pyroelectric measurements were made in the temperature range 300–800 K by employing the direct method of Byer–Roundy, using a programmable furnace in conjunction with an autoranging picoammeter (Keithley 485). Ferroelectric hysteresis loops were obtained on electrically poled samples, at a switching frequency of 50 Hz, using a modified Sawyer–Tower circuit.

III. RESULTS AND DISCUSSION

The n- and m-BiV powders were made into compacts of 10 mm diameter and 1–1.2-mm thickness, by applying a pressure of 60 MPa. Systematic investigations into the sintering behaviour of these powders[18] indicated that n-BiV powders show improved sintering characteristics, which can be related to the fine and uniform nature of the particles constituting these powders. Dense ceramics (>97% of the theoretical value) with almost uniform grain size (2 μm) could be obtained by sintering n-BiV compacts at a temperature as low as 993 K for 20 h (labeled as sample D), whereas m-BiV compacts required sintering at 1073 K for 24 h to achieve a density of 94% of the theoretical value. At this stage the grain size is ≈12 μm (sample A). Ceramic samples with grain sizes within the range 2–12 μm (samples B, C) were fabricated using powders which were heat-treated at different temperatures after mechanically activating for various durations. The details of the sample preparation conditions are listed in Table I. The dielectric constant of all the samples under study were corrected for porosity so as to ensure that the dielectric constant variation is not due to the variation in density. It is observed that the dielectric constant increases with decrease in grain size over the whole frequency range under study. The dielectric dispersion in the low-frequency region is higher for ceramics with finer grains than ceramics with coarser grains. The temperature variation of dielectric constant of samples A–D are shown in Fig. 1. It was observed that, as the grain size decreases, the dielectric constant systematically increases, both at room temperature and at the transition temperature. The nature of dielectric dispersion, of samples A and D, at the transition temperature at various frequencies is shown in Figs. 2(a) and 2(b), respectively. It is clear that the transition becomes broader at higher frequencies, in both cases. The temperature of highest dielectric constant does not change with frequency for sample A. However, for sample D, it shifts to higher temperatures with increase in frequency. The complex impedance analyses performed on these samples indicate that as the grain size reduces the grain boundary capacitance (C_{gb}) and resistance (R_{gb}) increase. The results of the impedance analyses are given in Table II. The increase of dielectric constant with decrease in grain size is unexpected, as our previous study[19] on the variation of dielectric constant with grain size (7–25 μm) had indicated that the dielectric constant of BiV ceramic increases with increases in grain size.

There are a number of reports on the dielectric constant variation with grain size in ceramics.[20–24] On comparison with other systems, the trend in the dielectric constant variation is quite different in the case of BiV. The ϵ_r value increases both at room temperature and at the transition point as the grain size reduces, for ceramics obtained from milled powders, while it increases with increase in grain size, in the case of ceramics obtained from m-BiV powders. So it is unlikely that the dielectric behavior is directly related to either the domain or the internal-stress effects.

The mechanism proposed to explain the dielectric behavior of these ceramics is based on the vanadium-reduced nature of these ceramic samples. Our preliminary studies concerning the influence of devia-

TABLE I. Sintering characteristics of samples milled for various durations.

Sample	Sample preparation conditions: Milling time (h)	Phase-formation temp. (K)	Sintering temp. (K)	Density (%)	Average grain size (μm)	$\epsilon_{r(RT)}$ (10 kHz)
A	0	1073	1073	95	12	132
B	16	903	1033	96	8	137
C	32	783	1013	96	5	141
D	54	RT	993	98	2	190

tions from the stoichiometry on the properties of BiV indicated that the phase transition temperature decreases and the dielectric constant increases both at room temperature and at the transition temperature with increase in vanadium reduction. The transition temperatures and the electrical characteristics of two samples X (unreduced-BiV) and Y (reduced-BiV) with almost same grain size and morphology are listed in Table III. Since the ball-milled powders have a large concentration of V^{4+},[25] the sintered ceramics obtained from these powders may contain a large amount of reduced-BiV. Indeed the electron paramagnetic resonance (EPR) studies carried out on these ceramics confirmed the presence of substantial amount of V^{4+}. Ceramics with finer grain sizes were fabricated from powders activated for longer durations and as a result, these are expected to have higher V^{4+} ion concentrations. The reduced-BiV phases (which are the impurity phases) have higher probability of segregating at the grain-boundaries. Therefore, the grain-boundaries are expected to be significantly modified in these ceramics. Indeed, the results of the complex impedance analyses (Table II) indicate that the grain-boundary capacitance (C_{gb}) and grain-boundary resistance (R_{gb}) values increase as the grain size reduces, thus supporting the above proposition. It implies that with reduction in grain size, there is not only an increase in the volume fraction of the grain boundaries but also an increase in the grain-boundary capacitance. However, in the case of ceramics obtained from nonmilled powders, coarser-grained ceramics have higher dielectric constants. This is because ceramics with coarser grain sizes have been prepared by sintering at higher temperatures and thus have higher concentrations of reduced-BiV (as evidenced by the change in color from brick red to grayish black and the increase in the EPR signal strength with increase in sintering temperature). This accounts for the increase in dielectric constant and dielectric dispersion with increase in grain size.

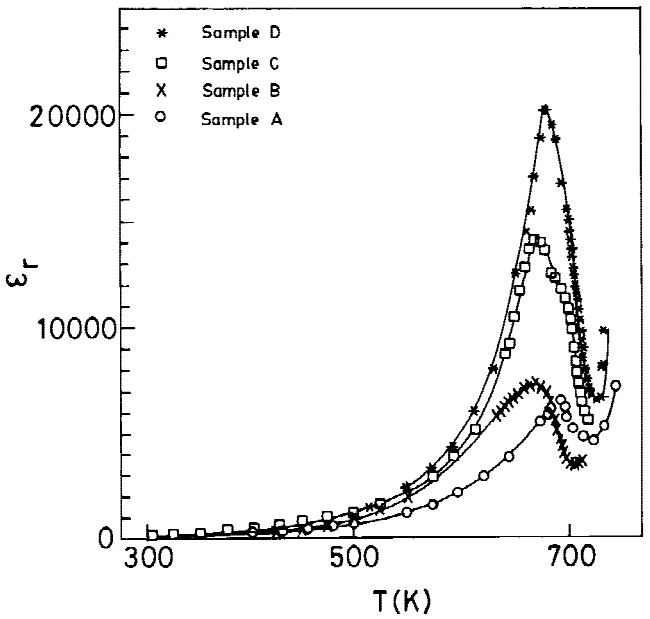

FIG. 1. Temperature dependence of ϵ_r of BiV ceramic samples A–D, recorded at 10 kHz.

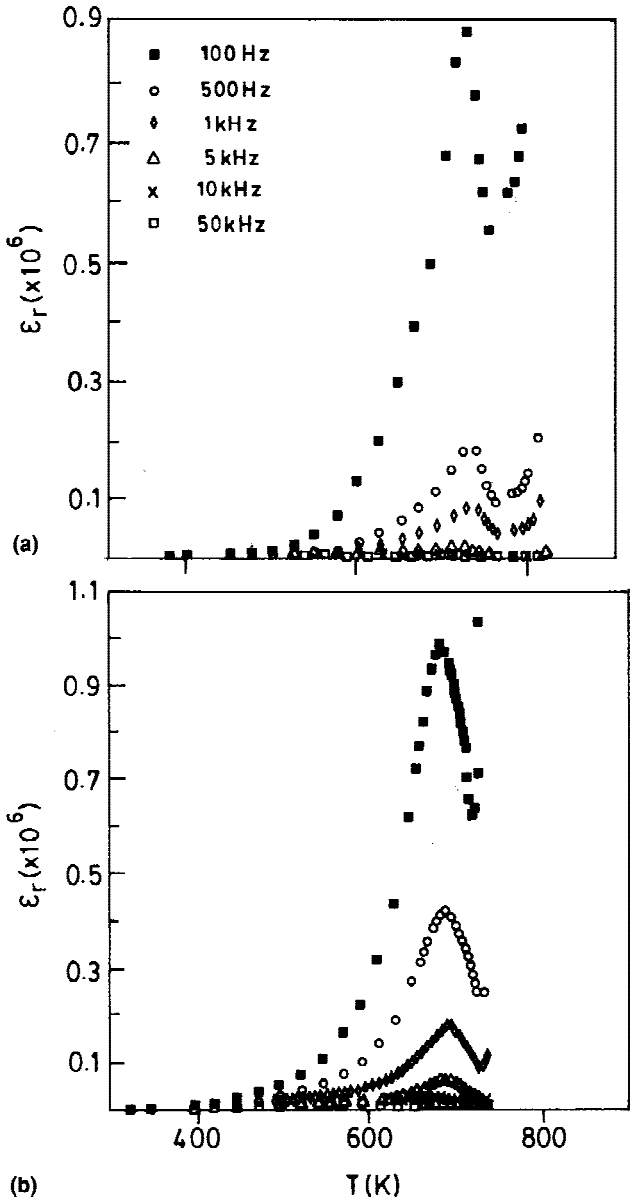

FIG. 2. Temperature dependence of ϵ_r recorded at various frequencies for samples (a) A and (b) D.

TABLE II. Grain and grain-boundary capacitance and resistance for samples A–D.

Sample	C_{gb} (F)	R_{gb} (Ω)	C_g (F)	R_g (Ω)
A	1.67×10^{-8}	5.69×10^{3}	3×10^{-10}	1.29×10^{3}
B	1.7×10^{-8}	7.6×10^{3}	2.56×10^{-10}	2.05×10^{3}
C	2.32×10^{-8}	3.17×10^{3}	2.7×10^{-10}	0.9×10^{3}
D	3.14×10^{-8}	1.89×10^{3}	3.17×10^{-10}	0.52×10^{3}

TABLE III. Transition temperature and electrical characteristics of samples X and Y.

	Sample X	Sample Y
T_c (K)	721	716
$\epsilon_{\tau RT}$ (10 kHz)	90	140
$(\epsilon_\Gamma)_{RT}$ (1 MHz)	80	132
$(\epsilon_\Gamma)_{T_c}$ (10 kHz)	3800	6500
$(\epsilon_\Gamma)_{T_c}$ (1 MHz)	280	310
C_g (520 K) (F)	1.27×10^{-10}	4.58×10^{-10}
C_{gb} (520 K) (F)	0.9×10^{-8}	2.13×10^{-8}
R_g (520 K) (Ω)	2.22×10^{3}	6.22×10^{2}
R_{gb} (520 K) (Ω)	1.96×10^{4}	1.22×10^{4}

Another important observation made in the present investigations is the broad ferroelectric–paraelectric transition in ceramics obtained from mechanically activated powders, unlike the nearly sharp transition exhibited by the conventionally fabricated ceramics. The nature of phase transition occurring in ferroelectric materials could be predicted from the plot of $1/\epsilon_r$ versus temperature. Figures 3(a)–3(d) shows the plot of $1/\epsilon_r$ (10 kHz) versus temperature for samples A–D, respectively. For sample A, a linear region is observed above the Curie point, implying that the dielectric constant obeys Curie–Weiss law at all temperatures above the transition. However for

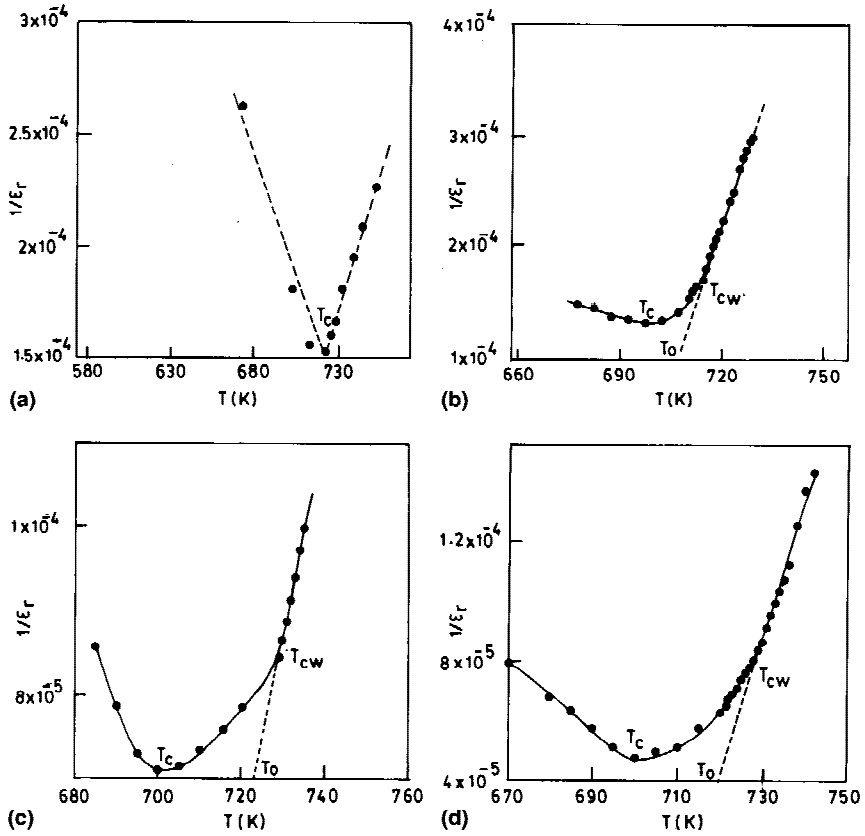

FIG. 3. Plot of $1/\epsilon_r$ (10 kHz) versus temperature for samples (a) A, (b) B, (c) C, and (d) D.

TABLE IV. Parameters T_c (K), T_c (K), and C_{cw} (K) estimated for samples B–D.

	Sample B			Sample C			Sample D		
Frequency	T_c (K)	T_o (K)	C_{cw} (K)	T_c (K)	T_o (K)	C_{cw} (K)	T_c (K)	T_o (K)	C_{cw} (K)
100 Hz	698	704	33×10^6	698	715	50×10^6	693	707	11.1×10^6
1 kHz	698	705	2.38×10^6	699	721	3.7×10^6	698	713	4.1×10^6
10 kHz	698	707	1.25×10^5	700	723	1×10^6	700	721	2.5×10^5
100 kHz	698	709	0.52×10^5	703	713	0.42×10^5	703	716	0.4×10^5
1 MHz	699	700	0.5×10^5	705	707	0.26×10^5	705	708	0.5×10^5

samples B–D, the curve can be divided into three regions; the first region represents the ferroelectric behavior until the transition T_c, the second region near the transition indicates a diffuse transition upto the temperature T_{cw}, and the third region represents the linear behavior of $1/\epsilon_r$ versus temperature in the paraelectric phase following the Curie–Weiss relation. It is clear from Figs. 3(b)–3(d) that, for $T > T_{cw}$, a normal Curie–Weiss behavior is found for all the samples. The difference, $\Delta T_m = T_{cw} - T_c$, is indicative of thermal diffuseness. The Curie–Weiss temperature, T_o, is obtained by extrapolating the third region on to the temperature axis, and the value of the Curie–Weiss constant (C_{cw}) is calculated from the slope of the curve in the third region. The constant T_o, T_c, C_{cw}, and T_{cw} were found to be frequency dependent for all the samples. These constants, calculated at various frequencies, for samples B–D are listed in Table IV.

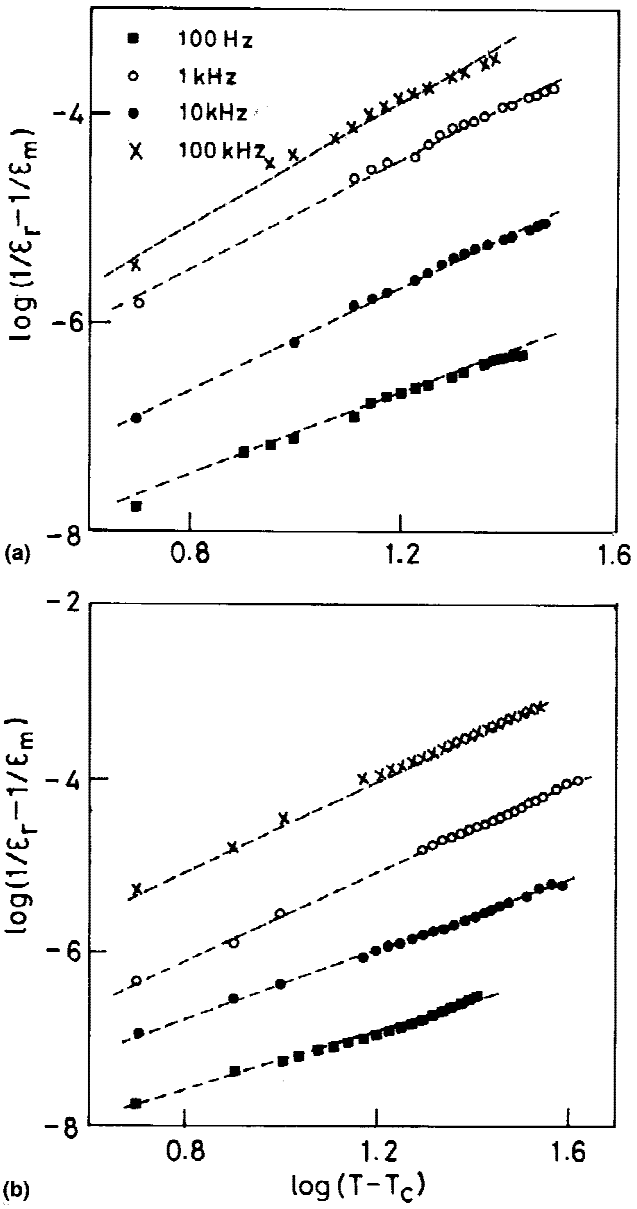

FIG. 4. Plot of log $(1/\epsilon_r - 1/\epsilon_{rm})$ versus log $(T - T_c)$, at four different frequencies, for samples (a) B and (b) D.

The above results confirm that the ferroelectric–paraelectric phase–transition exhibited by the ceramics obtained from mechanically activated powders is a diffused phase transition (DPT). On the basis of the Gaussian distribution of the composition and polarization fluctuation, the reciprocal of the dielectric constant and temperature obey the relation

$$1/\epsilon_r = 1/\epsilon_m + C'^{-1} (T - T_c)^{\gamma} \quad ,$$

where, C' is the Curie-like constant and γ is the critical exponent, taking the value between 1 (normal ferroelectric) and 2 (for a complete DPT).[26] A plot of log $(1/\epsilon_r - 1/\epsilon_m)$ versus log $(T - T_c)$ was generated, at different frequencies, for all the samples, in order to estimate the constants γ and C'. Using linear regression, the values of γ (the slope), the indicator of degree of diffuseness, and C' (from the intercept) were computed. Figures 4(a) and 4(b) show these plots for samples B and D. For the coarse-grained ceramic obtained using nonmilled powders (sample A) (not shown in the figure), the value of γ was found to be close to 1, suggesting that the transition follows Curie–Wiess law in the vicinity of T_c and there was no shift in T_c with frequency. Whereas, the samples obtained using mechanically activated powders (samples B–D) irrespective of their grain sizes yield γ values in the range 1.5–1.99 typical of a DPT.[27] These parameters estimated for samples B–D, at various frequencies, are listed in Table V. It is found that both C' and γ increase with increase in frequency; ΔT_m increases initially and then decreases with further increase in frequency (above

TABLE V. Parameters γ, ΔT_m, and C' estimated for samples B–D.

	Sample B			Sample C			Sample D		
Frequency	γ	ΔT_m	C'	γ	ΔT_m	C'	γ	ΔT_m	C'
100 Hz	1.93	10	1.09×10^8	1.511	19	4.46×10^7	1.9	19	1.58×10^8
1 kHz	1.96	13	1.35×10^7	1.928	20	4.1×10^7	1.978	23	2.46×10^7
10 kHz	1.98	17	8.13×10^5	1.932	29	3.85×10^6	1.98	28	1.32×10^6
100 kHz	1.99	13	0.12×10^5	1.933	10	3.4×10^6	1.99	20	2.38×10^5
1 MHz	1.90	5	0.2×10^5	1.94	3	0.28×10^5	1.92	5	0.10×10^5

50 kHz). The increase in γ with frequency suggests that the broadening effect is more pronounced at higher frequencies.

It is known that the mechanism of DPT in ferroelectric materials is generally associated with compositional inhomogeneities, or other structural defects.[28,29] The partial reduction in vanadium is likely to give rise to charged defects and compositional inhomogeneities in these samples. Diffuseness in the phase transition may be attributed to the irregular distribution of charged defects/impurities leading to the appearance of large-scale potential fluctuations. The ceramics obtained from milled powders consist of mixed-valence phases, with differing oxygen vacancy concentrations. It is observed that the phase transition temperature changes slightly with change in the amount of vanadium reduction in BiV ceramics. Therefore, the material can be assumed to be a congregate of microregions with different compositions which have slightly different T_c values. As a result, the phase transition is smeared over a temperature range rather than at a single temperature and, hence, the observed DPT behavior.

The pyroelectric coefficient of the ceramics obtained from milled powders is higher both at room temperature and at the transition temperature. They also exhibit improved hysteresis loops and better ferroelectric properties (with higher remnant polarization and lower coercive field). The data pertaining to the pyroelectric and ferroelectric characteristics of samples A and D are listed in Table VI, for comparison.

IV. CONCLUSION

In conclusion, the influence of preparation methods of BiV samples on their compositions, dielectric and polar properties, and the nature of phase transitions is clearly demonstrated. Ceramics obtained from powders subjected to mechanical activation exhibit superior dielectric characteristics and show diffused phase transition, unlike the conventionally prepared ceramics which exhibit normal sharp transition. These fine-grained ceramics obtained from mechanically activated powders with their better dielectric and polar properties are promising materials for polar device applications.

TABLE VI. Pyroelectric and ferroelectric characteristics of samples A and D.

	Sample A	Sample D
P_τ (C/cm^2)	2.25×10^{-8}	24.6×10^{-8}
E_c (V/cm)	650	480
P_{T_p} (mC/m^2 K)	140	2650
f_Q ($\times 10^6$ V m^{-1} K^{-1})	0.254	0.235

ACKNOWLEDGMENT

One of the authors (K.S.) thanks the CSIR, Government of India, for financial support.

REFERENCES

1. A.A. Bush and Y.N. Venevisev, Russ. J. Inorg. Chem. **31**(5), 769 (1986).
2. V.G. Osipian, L.M. Savchenko, V.L. Elbakyan, and P.B. Avakyan, Inorg. Mater. **23,** 467 (1987).
3. K.B.R. Varma, G.N. Subbanna, T.N. Guru Row, and C.N.R. Rao, J. Mater. Res. **5,** 2718 (1990).
4. K.V.R. Prasad and K.B.R. Varma, J. Phys. D: Appl. Phys. **24,** 1858 (1991).
5. K.V.R. Prasad and K.B.R. Varma, Mater. Chem. Phys. **38,** 406 (1994).
6. F. Abraham, M.L. De Gresse, G. Mairresse, and G. Nawogrocki, Solid State Ionics **28–30,** 529 (1988).
7. A. Cherrak, R. Hubaut, Y. Barbaux, and G. Mairresse, Catal. Lett. **15,** 377 (1992).
8. P.B. Avakyan, M.D. Nersesyan, and A.G. Merzhanov, Am. Ceram. Soc. Bull. **75**(2), 50 (1996).
9. P. Shuk, H-D. Wiemhofer, U. Guth, W. Gopel, and M. Greenblatt, Solid State Ionics **89,** 179 (1996).
10. M.E. Arroyo y de Dompablo, F. Garcia-Alvarado, and E. Moran, Solid State Ionics **91,** 273 (1996).
11. W. Heywang, Solid State Electron. **3,** 51 (1962).
12. J. Portelles, I. Gonzales, A. Kiriev, F. Calderon, and S. Garcia, J. Mater. Sci. Lett. **12,** 1871 (1993).
13. V. Tolmer and G. Desgardin, J. Am. Ceram. Soc. **80,** 1981 (1997).
14. S. Tashiro, N. Sasaki, Y. Tsuji, H. Igarashi, and K. Okazaki, Jpn. J. Appl. Phys. **26**(2), 142 (1987).
15. X. Li and W.H. Shih, J. Am. Ceram. Soc. **80,** 2844 (1997).
16. C.W. Nan and D.R. Clarke, J. Am. Ceram. Soc. **79,** 3185 (1996).
17. O. Joubert, A. Jouanneaux, and M. Ganne, Nucl. Instrum. Meth. Phys. Res. Sect. B. **97,** 119 (1995).
18. K. Shantha and K.B.R. Varma, J. Am. Ceram. Soc. (1999, in press).
19. K.V.R. Prasad, A.R. Raju, and K.B.R. Varma, J. Mater. Sci. **29,** 2691 (1994).
20. W.R. Buessem, L.E. Cross, and A.K. Goswami, J. Am. Ceram. Soc. **49,** 33 (1966).
21. H.T. Martirena and J.C. Burfoot, J. Phys. C: Solid State Phys. **7,** 3182 (1974).
22. T. Kanata, T. Yoshikawa, and K. Kubota, Solid State Commun. **62**(11), 765 (1987).
23. G. Arlt, D. Hennings, and G. de With, J. Appl. Phys. **58,** 1619 (1985).
24. L.E. Cross, Ferroelectrics **151,** 305 (1994).
25. K. Shantha and K.B.R. Varma, J. Mater. Sci. Eng. B (1999, in press).
26. K. Uchino and S. Nomura, Ferroelectr. Lett. **44,** 55 (1982).
27. B. Jimenez, J. De Frutos, and C. Alemany, J. Phys. Chem. Solids **48**(10), 877 (1987).
28. A.E. Krumins, Ferroelectr. Lett. **1,** 89 (1983).
29. L.A. Shebanov and L.V. Korzuneva, Mater. Res. Bull. **20,** 781 (1985).